Optogenetically-controlled TrkA Activity Improves the Regenerative Capacity of Hair-follicle-derived Stem Cells to Differentiate into Neurons and Glia

Taida Huang[1], Yan Zhang[2], Zitian Wang[3], Yunxin Zeng[1], Nan Wang[1], Huaxun Fan[4], Zhangsen Huang[1], Yixun Su[1], Xiaomin Huang[1], Hui Chen[5], Kai Zhang[4]*, Chenju Yi[1]*

[1]The Seventh Affiliated Hospital of Sun Yat-sen University, Shenzhen, 518107, China;

[2]Department of Orthopedics, Tianjin Medical University General Hospital, Tianjin, 300052, China;

[3]Tsinghua-Berkeley Shenzhen Institute, Tsinghua University, Shenzhen, 518055, China;

[4]Department of Biochemistry, School of Molecular and Cellular Biology, University of Illinois at Urbana-Champaign, Urbana, IL 61801, USA;

[5]School of Life Sciences, Faculty of Science, University of Technology Sydney, PO Box 123, Broadway NSW 2007, Australia.

* Corresponding author:

Kai Zhang (kaizkaiz@illinois.edu); Chenju Yi (yichj@mail.sysu.edu.cn)

Abstract

Hair-follicle-derived stem cells (HSCs) originating from the bulge region of the mouse vibrissa hair follicle are able to differentiate into neuronal and glial lineage cells. The Tropomyosin receptor kinase A (TrkA) receptor that is expressed on these cells plays key roles in mediating the survival and differentiation of neural progenitors as well as in the regulation of the growth and regeneration of different neural systems. In this study, we introduce the OptoTrkA system, which is able to stimulate TrkA activity via blue-light illumination in HSCs. This allows us to determine whether TrkA signaling is capable of influencing the proliferation, migration and neural differentiation of these somatic stem cells. We found that OptoTrkA was able to activate downstream molecules such

as ERK and AKT with blue-light illumination, and subsequently able to terminate this kinase activity in dark. HSCs with OptoTrkA activity showed an increased ability for proliferation and migration and also exhibited accelerated neuronal and glial cell differentiation. These findings suggest that the precise control of TrkA activity using optogenetic tools is a viable strategy for the regeneration of neurons from HSCs, and also provides a novel insight into the clinical application of optogenetic tools in cell-transplantation therapy.

1. Introduction

Different types of stem cells are being widely investigated in cell-transplantation and regenerative therapies for neural defects caused by congenital and acquired pathologies[1-4]. However, the route to the clinic for such cell-based therapies is a long one due to prevalent issues such as alloimmune rejection, the availability of cell sources and the potential long-term risk for tumorigenesis[4-6]. Hair follicles are an easily accessible structure on the skin and the stem cells harbored within them can consistently undergo self-renewal.[7,8] Hair-follicle-derived stem cells (HSCs) isolated from the bulge region of hair follicles were able to differentiate into neuronal and glial cells *in vitro* and also regenerate neurons in animal recipients[8-10]. HSCs are an ideal cell source for neural regeneration not only due to its differentiation potency to neural cell types, but also its reduced tumorigenicity as somatic stem cells, easy accessibility, as well as its lower rate for immunologic rejection during autologous transplantation.

Neurotrophin signaling is a key process that determines neural stem cell function, influencing cell survival, cell division and differentiation. These effects carry on to modulate functions in fate-determined cells, such as axonal and dendritic growth of neurons, cell death, neurotransmitter secretion and neuronal activity[11]. Neurotophin signaling is traditionally mediated through ligand

binding to the Trk receptor tyrosine kinase family and, with less affinity, to the p75 neurotrophin receptor[11-13]. Although Trk receptors have been investigated in a variety of different cell types, little is known about its function in HSCs during neural differentiation. As key Trk-mediated effects such as active proliferation, cellular migration and differentiation are critical processes in cell graft survival and its ability to fully regenerate neurons after transplantation, various groups have examined the effect of Trk receptors activation in a variety of neural progenitors by using techniques such as genetic overexpression or by agonist-induced activation of the receptor[13-15]. However, these approaches are not feasible for clinical applications. One major issue is that certain receptors such as TrkC can act as an oncogene in a variety of tumor cells, and manipulation of *TrkC* over-expression using genetic methods has been acknowledged to result in an extremely high tumorigenic potential. Furthermore, manipulation of exogenous Trk activity using such methods results in receptor levels persisting in a non-physiological manner even after neuronal differentiation. Also, using small-molecule agonists of Trk receptors has its own caveats; a plethora of unknown off-target effects suggests that rigorous testing before clinical use will be required[16,17]. Therefore, strategies that can enact precise control on the activities of Trk receptors in HSCs such as through some form of "biochemical switch" need to be developed in order to manipulate neural regeneration efficiency in these cells, with the condition that such a switch must be able to terminate Trk activity after regeneration processes to ensure that levels of Trk receptors can be restored to physiological levels after fate-determination.

Emerging cutting-edge optogenetic techniques allow for spatiotemporal regulation of the activity of single molecules[18-21]. Previously, we developed an optogenetic tool (OptoTrkA) that allows reversible activation of TrkA signaling by the fusion of the intracellular domain of TrkA (TrkA-ICD) with the light-oxygen-voltage domain of aureochrome 1 from *Vaucheria frigida*

(AuLOV)[18]. We expect that OptoTrkA is only activated after excitation by light and this activation is spontaneously resolved in the dark and activation of TrkA using the OptoTrkA system will influence the proliferation, migration and neural differentiation (to neuronal and glial cell types) of HSCs.

In this study, we used the OptoTrkA system within primary cultured HSCs isolated from mouse vibrissa hair follicles and found that light induced TrkA activity was able to promote cell proliferation, migration and differentiation into neuronal and glial cells *in vitro*. The results of our study demonstrated the optogenetically-controlled TrkA activity in HSCs and revealed the functional role of TrkA in driving the neurogenesis of HSCs.

2. Results

2.1. Optogenetic Activation of TrkA in HSCs

Previously, we developed an optogenetic system (OptoTrkA) that allows for TrkA activation upon controlled light excitation (Figure 1A and 1B). This system was constructed by fusing the intracellular domain of TrkA (TrkA-ICD) with the light-oxygen-voltage domain of from *Vaucheria frigida* aureochrome 1 (AuLOV). Upon light excitation, the homo-association of AuLOV pulls two copies of TrkA-ICD within close proximity and further initiating its cross- and autophosphorylation (Figure 1B). HSCs originated from bulge region of mouse vibrissa hair follicle were primary cultured *in vitro* and transfected with the plasmid expressing OptoTrkA (Figure 1C). HSCs with OptoTrkA transfection were subjected to cellular analyses, including BrdU staining, wound-healing assay, directed differentiation analysis, etc. in order to determine the functional effects of TrkA on the proliferation, migration and neural differentiation of HSCs (figure 1D).

2.2. Isolation and Characterization of HSCs

Mouse vibrissa hair follicle explants were isolated according to the procedure as described in the Methods (Figure 2A, i-iv). After the culture of mouse follicle explants, we found that proliferative cells migrate outward from the explant in migration medium after 2-3 days, whereupon the explant was removed on Day 4 (Figure 2B). In general, we found that cell numbers ranged from between 8,000 to 10,000 per explant when cultured in expansion medium on Day 7 whereupon these cells were enzymatically dissociated for passaging (Figure 2B). Characterization of primary cultured cells was performed by immunofluorescence staining of markers such as Nestin, p75, Sox10 and Oct4. We found that early migrated cells (Day 3) expressed markers such as Nestin, p75 and Sox10 (Figure 2C). After passaging, sub-cultured cells were found to also be Nestin and Oct4 double immunoreactive (Figure 2D). In addition, we isolated mRNA from these cells and were able to detect the expression of stem cell markers such as *Oct4*, *Sox2* and *Nanog* by reverse-transcription PCR (Figure 2E). Meanwhile, we also found that expression of neural stem cell markers, including *Nes* (encoding Nestin) *Sox9*, *Sox10* and *Ngfr* (encoding $p75^{NTR}$), were also found to be expressed in these cells (Figure 2E). In summary, the cells isolated from mouse vibrissa hair follicle exhibited markers of stem cells, especially neural stem cells, which were similar to the hair-follicle-derived stem cells (HSCs) reported previously [7,9,10]; thus, we also termed these cells as HSCs in our present study.

2.3. Light-stimulated OptoTrkA Activity Enhances the Proliferation and Migration of HSCs

Previous studies have reported that TrkA selectively promotes cell proliferation and migration or may even result in cell death pathway activation in a variety of cell types[16,22-24]. To determine whether blue light-induced OptoTrkA activity has any effect on the proliferation and migration of

HSCs, we introduced OptoTrkA into primary cultured HSCs. This was followed by BrdU staining to examine proliferation and a wound healing assay to examine cellular migration. HSCs with light-induced activation of OptoTrkA (pOptoTrkA-light) showed a significantly higher percentage of BrdU immunoreactivity as compared with those HSCs in pEGFP-dark, pOptoTrkA and pOptoTrkA-dark groups, which suggests that activation of OptoTrkA was able to increase the proliferation of HSCs (Figure 3A and 3B). In the wound healing assay, HSCs with blue light-activated OptoTrkA showed a significantly higher ability to migrate into the wound over a period of 12h and 24h when compared to the other three control groups (Figure 3C and 3D). By counting the average distance between each cell to its closest neighbor at the 24h time point, we found that HSCs were more dispersed in the light-activated OptoTrkA group as compared to the cells in other groups (Figure 3E). We also performed the TUNEL assay and Caspase-3 staining of HSCs with and without OptoTrkA activity and found no significant difference in cell apoptosis or cell death (supplementary figures). These gain-of-function studies of OptoTrkA therefore suggest that the proliferation and migration of HSCs could be enhanced by the light-induced activation of OptoTrkA *in vitro*.

2.4. Light-induced Activation of OptoTrkA can Boost Neuronal Cell Differentiation of HSC

To determine whether activated OptoTrkA can improve HSC neuronal cell differentiation, we performed a directed differentiation protocol followed by immunofluorescence staining of neuronal markers. pOptoTrkA was transfected into primary cultured HSCs, and these HSCs were induced into neurons in neuronal cell differentiation medium. By examining neuronal markers Tuj1, PGP9.5 and Map2, we found that all the HSCs in four different groups were able to differentiate into neurons (Figure 4A, 4D and Supplementary Figure 1A). However, the activated OptoTrkA group had a

significantly higher percentage of Tuj1 and PGP9.5 immunoreactive cells as compared to those in the control groups (Figure 4B and 4E). To further confirm that activation of OptoTrkA can promote neuronal cell differentiation, we analyzed the number of neuronal cells, which showed a fibrous cell structure. We found that the HSCs with activated OptoTrkA were able to show a higher percentage of cells with fibrous morphology as compared to the controls (Figure 4C and 4F). These findings reveal that OptoTrkA not only promotes the neuronal differentiation of HSCs but also can accelerate the maturation of neuronal cells.

2.5. Light-induced Activation of OptoTrkA can Enhance Glial Cell Differentiation of HSCs

Next, we sought to further understand if the light-induced activation of OptoTrkA could also promote glial cell differentiation of HSCs. A similar protocol to our neuronal cell differentiation protocol was used, but differentiation was induced by using a glial cell induction medium. In these experiments, we found that HSCs with activated OptoTrkA showed a significantly higher percentage of glial differentiation as determined by immunofluorescence staining of Fabp7 (Figure 5A and 5B) and S100b (Figure 5D and 5E), but not of GFAP (an astrocyte marker, Supplementary figure 1C and 1D). In addition, higher fluorescence intensity of Fabp7, S100b and GFAP was detected in the HSCs with activated OptoTrkA as compared with those in the control groups (Figure 5C, 5F and Supplementary figure 1E). In conclusion, light-activated OptoTrkA was able to enhance the glial cell differentiation of primary cultured HSCs.

2.6. OptoTrkA can be Stimulated by Blue-light Exposure and Spontaneous Deactivated in the Dark

To interrogate whether OptoTrkA is only activated by blue-light exposure, we performed Western

blotting to examine the phosphorylation of downstream signaling pathways regulated by TrkA, including ERK and AKT protein. We transfected the OptoTrkA protein expression plasmid (pOptoTrkA) into HEK293T cells *in vitro* and stimulated OptoTrkA activity by using blue-light illumination cycles for 12 hours (0.2 mW/cm^2) (Figure 6A). Along the treatment group (pOtpoTrkA-light), three control groups were set up: cells infected with pEGFP-N1 vector and maintained in the dark (pEGFP-dark); cells infected with pOptoTrkA plasmid and maintained in the dark (pOptoTrkA-dark), and cells infected with pEGFP-N1 and illuminated with blue light (pEGFP-light). Western blotting showed that blue light stimulated optogenetic TrkA led to increased phosphorylation of ERK1/2 (p-Thr202/Try204) and AKT (p-Ser473) in HEK293T cells, however, illumination of EGFP only controls or OptoTrkA without illumination did not have a significant effect on activating ERK and AKT signaling pathways (Figure 6B, 6C and 6D).

Thereafter, the four experimental groups were all equally placed into the dark for another 24 hours to spontaneously deactivate OptoTrkA stimulation. Phosphorylation of ERK1/2 and AKT was determined again by Western blotting. No significant differences in p-ERK1/2 and p-AKT could be detected in the OptoTrkA-light cells when compared to that in the other three control groups which did not have both pOptoTrkA and prior illumination (Figure 6E, 6F and 6G). Taken together, this data suggests that OptoTrkA can be stimulated to activate downstream ERK and AKT signal pathways using blue-light illumination, and this can be spontaneously converted back to an inactivated state when placed into the dark.

3. Discussion

The overall goal of this study is to determine whether stimulation of TrkA activity controlled by

185 blue light illumination is able to improve cell proliferation, differentiation and neural differentiation
186 of HSCs. Towards this goal, we developed an optogenetic tool to stimulate TrkA activity in HSCs
187 and deciphered the function of TrkA in these somatic stem cells. We found that light-induced
188 activation of OptoTrkA was able to promote the proliferation of HSCs, which suggests that
189 manipulation of TrkA activation in HSCs has the potential to improve cell survival and increase the
190 population size of cell grafts after transplantation. Second, HSCs with OptoTrkA activity also
191 showed enhanced migratory ability, which has the effect of improving cell grafts colonization in
192 transplant recipient tissue where there is a need to regenerate neurons in large areas or across long
193 distances. Third, HSCs with activated OptoTrkA demonstrated a significantly accelerated neural
194 differentiation towards neuronal and glial lineages. These results suggest that stimulating TrkA
195 activity using optogenetic tools in HSCs is a viable therapeutic strategy to regenerate neural defects
196 in future clinical applications.

197 TrkA, together with TrkB, TrkC and $p75^{NTR}$, participate in mediating neurotrophin (NT)
198 signaling. Of the traditional neurotrophic factors, NGF binds TrkA, BDNF and NT-4/5 binds to
199 TrkB, NT-3 binds to TrkC, though all neurotrophic factors are also able to bind to low-affinity
200 neurotrophin receptor $p75^{NTR}$[11,25,26]. The downstream pathways from Trk receptors share many
201 common protein substrates such as the Ras/Mapk/Erk, PLCγ, and PI3K/AKT signaling
202 pathways[24,25]. To our present knowledge, ERK1/2 plays a key role in neuronal survival and axonal
203 maintenance after neural damage[27,28], and the AKT signaling pathway controls cytoskeletal
204 dynamics for axon elongation and cell migration during neural regeneration[14,29,30]. We found that
205 OptoTrkA is able to significantly activate both ERK1/2 and AKT pathways, which we determined
206 using phosphorylation of ERK1/2 (p-Thr202/Try204) and AKT (p-Ser473) in our western blotting
207 assay (Figure 3). Previous studies by our group and others have shown that two tyrosine residues,

Y490 and Y785, which are located within the intracellular domain of TrkA, serve as the primary phosphorylated sites for triggering downstream ERK1/2, AKT and PLCγ activation during neuronal differentiation in PC12 cells[18,31,32]. However, even though the functional mechanism of TrkA in HSCs still remains unclear, similar molecular interactions in PC12 may also exist in HSCs. Therefore, specific phosphorylation inhibitors such as U0126 which targets ERK1/2 and LY294002 which targets AKT may help to interrogate the detailed protein-protein interactions during TrkA activation in HSCs and can be used for further studies.

Multipotent stem cells isolated from hair and skin have been successfully used for cell-transplantation therapy in spinal cord-injured and neonatal shivered mice[33-35]. High throughput profiling by RNA sequencing showed that the neural progenitors from both rodent and human hair follicles have gene expression signatures similar to those of the mouse neural crest stem cells and human neuronal cells[36,37]. HSCs, therefore, are a good target for further studies into genetic modifications and clinical applications in regenerative medicine towards repairing neural defects. Enlightened by the previous findings that show that Trk receptor activation can significantly increase the survival rate and neural regeneration efficiency in stromal cell transplantation[13-15,23], we activated TrkA in HSCs and determined that modulating TrkA activity has beneficial roles in improving proliferation, migration and neural differentiation. As Trk signaling has previously been identified in various solid tumors[16,17], we used a cautious approach to stimulate TrkA activity via optogenetic tools which are only active during light illumination to effectively reduced the long-term tumorigenic risk. Moving this approach to the clinic is aided by the fact that novel nanometer materials to facilitate deep-tissue light delivery have seen significant improvement in the last decade[38-40]. Therefore, *in vivo* investigation of TrkA activation in HSCs by optogenetic control for regenerating neurons is a viable next step in improving neural regeneration after transplantation.

4. Conclusion

In conclusion, we have provided evidence that shows that TrkA activation promotes cell proliferation, migration and neural differentiation of stem cells isolated from the bulge region of mouse vibrissa hair follicle. In addition, with optogenetic tools, TrkA signaling activity can be precisely controlled by blue light illumination. It is hoped that our work will bring a novel angle to cell-transplantation therapy using somatic stem cells for neural regeneration.

5. Experimental Section

Animals: Wild-type C57BL/6J mice were purchased from the Jackson Laboratory. All mice were maintained on an artificial 12/12 hours light/dark cycle. Ethical approval for all animal procedures was obtained from the Sun Yat-Sen University Institutional Animal Care and Use Committee (Approval No. SYSU-IACUC-2020-B0538).

Cell culture: The adult mice (6-8 weeks) were sacrificed by cervical dislocation. The mouse head was sterilized for 1-2 min in a solution consisting of a 50% hydrogen peroxide and a 5% povidone-iodine solution. The whisker pads were dissected and immersed in 1× Dulbecco's phosphate-buffered saline (DPBS). The vibrissa hair follicles from the whisker pads were then further dissected by removing the hair dermis, the papilla sebaceous gland and the connective tissue capsule. A single explant containing HSCs was cultured in α-MEM medium (Gibco, 32571) containing 10% fetal bovine serum (FBS) (Gibco, 16000044). Coverslips for explant culture were coated with 20 μg/ml collagen type I (BD,354236). After 3 days in culture, the hair follicle explants were removed and emigrated HSCs were further cultured in cell expansion medium which contains DMEM/F12 (Gibco, 1133032), 10% FBS, 1x B27 supplement, 10 ng/ml fibroblast growth factor

(FGF) (Gibco, PHG0266-25), epidermal growth factor (EGF) (Gibco PHG0311), glial cell-derived neurotrophic factor (GDNF) (R&D System, 212-GD). Primary-cultured HSCs were dissociated and passaged using Accutase (Millipore, SCR005) on Day 7.

Differentiation tests: To induce the differentiation of HSCs into neuronal cells, the cells were transferred to a modified neuronal differentiation medium containing DMEM/F12, 1×B27 supplement (Gibco, 17504-044), 1×N2 supplement (Gibco,17502-048), 20 ng/ml BMP2 (Gibco, PHC7145), and 1 μM all-trans-retinoic acid (Sigma, R2625) for 3 days. To induce differentiation of HSCs into glial cells, the cells were transferred to a modified glial differentiation medium containing DMEM/F12, 2 mM L-glutamine (Gibco, 25030081), 2 ng/ml insulin (Sigma, I1882), 1×B27 supplement (Gibco, 17504-044), 1×N2 supplement (Gibco, 17502-048), and 50 ng/ml BMP2 (Gibco, PHC7145) for 3 days.

Plasmid construction and transfection: The OptoTrkA plasmid was constructed as previously described[18]. Cells were transfected using Lipofectamine Stem Transfection Reagent (Invitrogen, STEM00008) following the manufacturer's instructions. Successful transfection was confirmed by fluorescence microscopy 24 h post-transfection.

Light stimulation: The instrument used for blue light illumination was described previously[18]. To stimulate TrkA activity using blue light in HSCs, a 12-well plate containing OptoTrkA-transfected cells was illuminated on a 10/50 minutes on/off cycle. The light intensity was adjusted to 0.2 mW/cm^2 at the position of the cells.

Immunofluorescent staining and western blotting: Cells grown on collagen type I-coated coverslips were fixed with 4% paraformaldehyde for 15min at room temperature followed by 3 rounds of PBS rinsing at 10 min each, The cells were then blocked using 1% BSA (Sigma, 9418) in PBS containing 1% Triton X-100 (USB, 22686) for 1h. Primary antibodies (Table 1) were diluted

at the manufacturer's recommended dilution ratio in blocking buffer and incubated with the cells at 4°C overnight. Secondary antibodies were diluted at a ratio of 1:300 in blocking buffer for 1h at room temperature. After washing 3 times in PBS containing 0.5% Tween-20 (USB, 20605), cells were counter-stained with 0.15% (w/v) DAPI (Sigma, 9542) in PBS and mounted using FluorSave Reagent (Millipore, 345789). Fluorescent images were photographed using an epifluorescence microscope (Olympus). For BrdU assays, BrdU reagent was added into culture medium 2h prior to fixation, after which genomic DNA was denatured using 2N HCl for 30 min at room temperature to expose BrdU-labelled DNA before following standard immunostaining protocols. For Western Blotting, cells were lysed in RIPA buffer (CST, 9806) containing PMSF (Sigma, 10837091001) and cOmplete™ Protease Inhibitor Cocktail (Roche, 11697498001) on ice for 10 min, followed by centrifugation at 12,000g for 10 min to remove the insoluble fraction. Protein concentration was measured using the BCA kit (Pierce, 23227). Protein samples were then equalized by dilution in SDS sample buffer and then boiled at 99°C for 5 min before SDS-PAGE. Samples on the acrylamide gel were transferred to activated PVDF membranes (Bio-Rad, 162-0184) and immunoblotted using primary antibodies diluted in 5% BSA:TBST at a ratio of 1:1000, followed by appropriate HRP-conjugated secondary antibodies (diluted at 1:10,000), and finally developed by using the Clarity Western ECL substrate (Bio-Rad, 170-5060).

Wound healing and cell dispersion assay: A cell-free area for wound healing assay was created by physical exclusion using a commercialized culture insert (ibidi, 81176) following the manufacturer's protocol. To avoid interference from cell proliferation, cells were starved in serum-free DMEM/F12 medium. Images of all groups were taken at 12h, 24h and 36h. At the 12h timepoint, cells that migrated into the cell-free area in each group were selected for the cell dispersion assay by measuring the distance of each cell to its closest neighbor.

Statistical Analysis: The ImageJ software was used for image analysis, including the quantification of cell distance, cell number and fluorescence intensity. All quantitative results were displayed as the mean ± S.D. Statistical significance was assessed using non-parametric ANOVA (Kruskal-Wallis with Dunn's multiple comparisons post-test) using Prism 7 (GraphPad). Statistical significance was set at $p<0.05$ with a 95% confidence interval.

Author contribution

Taida Huang: Conceptualization, Methodology, Visualization, Investigation, Writing - Original Draft. Yan Zhang and Zitian Wan: Visualization. Yunxin Zeng: Editing. Nan Wang: Visualization, Investigation. Huaxun Fan: Methodology. Zhangsen Huang, Yixun Su and Xiaomin Hunag: Investigation. Hui Chen: Validation. KZ: Supervision, Methodology. CY: Supervision, Writing – Review & Editing.

Acknowledgements

This work was supported by grants from the National Nature Science Foundation of China (NSFC 81971309), Guangdong Basic and Applied Basic Research Foundation (2019A1515011333) and the Fundamental Research Funds for the Central Universities (F7201931620002).

Keywords

Hair-follicle-derived stem cells, optogenetically-controlled TrkA activity, proliferation, migration,

neuronal and glial differentiation

Reference

[1] S. Yi, Y. Zhang, X. K. Gu, L. Huang, K. R. Zhang, T. M. Qian, X. S. Gu, *Burns. Trauma.* **2020**, *8*, tkaa002.

[2] H. Atkins, *Jama-J. Am. Med. Assoc.* **2019**, *321*, 153.

[3] T. K. Watanabe, *Pm&R.* **2018**, *10*, S151.

[4] Z. B. Jin, M. L. Gao, W. L. Deng, K. C. Wu, S. Sugita, M. Mandai, M. Takahashi, *Prog. Retin. Eye. Res.* **2019**, *69*, 38.

[5] K. M. Haston, S. Finkbeiner, *Annu. Rev. Pharmacol.* **2016**, *56*, 489.

[6] F. A. Khan, D. Almohazey, M. Alomari, S. A. Almofty, *Stem. Cells. Int.* **2018**, *2018*, 1429351.

[7] M. Call, E. A. Meyer, W. W. Kao, F. E. Kruse, U. Schlotzer-Schrehardt, *Bio-Protocol.* **2018**, *8*, e2848.

[8] A. Owczarczyk-Saczonek, M. Krajewska-Wlodarczyk, A. Kruszewska, L. Banasiak, W. Placek, W. Maksymowicz, J. Wojtkiewicz, *Stem. Cells. Int.* **2018**, *2018*, 1049641.

[9] C. G. Gho, T. Schomann, S. C. de Groot, J. H. M. Frijns, M. N. Rivolta, M. H. A. Neumann, M. A. Huisman, *Cytotechnology,* **2016**, *68*, 1849.

[10] K. Obara, N. Tohgi, S. Mii, Y. Hamada, N. Arakawa, R. Aki, S. R. Singh, R. M. Hoffman, Y. Amoh, *Sci. Rep-Uk.* **2019**, *9*, 9326.

[11] L. M. Maness, A. J. Kastin, J. T. Weber, W. A. Banks, B. S. Beckman, J. E. Zadina, *Neurosci. Biobehav. R.* **1994**, *18*, 143.

[12] E. M. Wexler, O. Berkovich, S. Nawy, *Vis. Neurosci.* **1998**, *15*, 211.

[13] S. Pramanik, Y. A. Sulistio, K. Heese, *Mol. Neurobiol.* **2017**, *54*, 7401.

[14] M. G. Zheng, W. Y. Sui, Z. D. He, Y. Liu, Y. L. Huang, S. H. Mu, X. Z. Xu, J. S. Zhang, J. L. Qu, J. Zhang, D. Wang, *Neural. Regen. Res.* **2019**, *14*, 1765.

[15] D. A. Castellanos, P. Tsoulfas, B. R. Frydel, S. Gajavelli, J. C. Bes, J. Sagen, *Cell Transplant.* **2002**, *11*, 297.

[16] J. Meldolesi, *Rev. Physiol. Biochem. Pharmacol.* **2018**, *174*, 67.

[17] A. M. Lange, H. W. Lo, *Cancers (Basel).* **2018**, *10*, 105.

[18] J. S. Khamo, V. V. Krishnamurthy, Q. Chen, J. Diao, K. Zhang, *Cell. Chem. Biol.* **2019**, *26*, 400.

[19] B. Kim, M. Z. Lin, *Biochem. Soc. Trans.* **2013**, *41*, 1183.

[20] K. Muller, S. Naumann, W. Weber, M. D. Zurbriggen, *Biol. Chem.* **2015**, *396*, 145.

[21] D. Tischer, O. D. Weiner, *Nat. Rev. Mol. Cell. Bio.* **2014**, *15*, 551.

[22] E. J. Jung, D. R. Kim, *Mol. Cells.* **2008**, *26*, 12.

[23] J. Luzuriaga, J. R. Pineda, I. Irastorza, V. Uribe-Etxebarria, P. Garcia-Gallastegui, J. M. Encinas, P. Chamero, F. Unda, G. Ibarretxe, *Cell. Physiol. Biochem.* **2019**, *52*, 1361.

[24] D. R. Kaplan, F. D. Miller, *Curr. Opin. Cell. Biol.* **1997**, *9*, 213.

[25] A. Patapoutian, L. F. Reichardt, *Curr Opin Neurobiol,* **2001**, *11*, 272.

[26] W. J. Friedman, L. A. Greene, *Exp Cell Res,* **1999**, *253*, 131.

[27] V. Waetzig, T. Herdegen, *Mol. Cell. Neurosci.* **2005**, *30*, 67.

[28] Y. Tsuda, M. Kanje, L. B. Dahlin, *Bmc Neurosci.* **2011**, *12*, 12.

[29] L. Klimaschewski, B. Hausott, D. N. Angelov, *Int. Rev. Neurobiol.* **2013**, *108*, 137.

[30] A. Markus, J. Zhong, W. D. Snider, *Neuron.* **2002**, *35*, 65.

[31] J. Biarc, R. J. Chalkley, A. L. Burlingame, R. A. Bradshaw, *J. Biol. Chem.* **2013**, *288*, 16606.

[32] A. Obermeier, R. A. Bradshaw, K. Seedorf, A. Choidas, J. Schlessinger, A. Ullrich, *Embo. J.*

1994, *13*, 1585.

[33] I. A. McKenzie, J. Biernaskie, J. G. Toma, R. Midha, F. D. Miller, *J. Neurosci.* **2006**, *26*, 6651.

[34] Y. Amoh, M. Kanoh, S. Niiyama, K. Kawahara, Y. Sato, K. Katsuoka, R. M. Hoffman, *Cell Cycle.* **2009**, *8*, 176.

[35] M. Sieber-Blum, L. Schnell, M. Grim, M. E. Schwab, *Faseb. J.* **2006**, *20*, A441.

[36] H. Yu, S. M. Kumar, A. V. Kossenkov, L. Showe, X. W. Xu, *J. Invest. Dermatol.* **2010**, *130*, 1227.

[37] S. Joost, K. Annusver, T. Jacob, X. Y. Sun, T. Dalessandri, U. Sivan, I. Sequeira, R. Sandberg, M. Kasper, *Cell Stem Cell.* **2020**, *26*, 441.

[38] S. Chen, X. G. Liu, T. McHugh, *Proc. Spie.* **2019**, *10873*, 679

[39] Y. W. Zhang, L. Huang, Z. J. Li, G. L. Ma, Y. B. Zhou, G. Han, *Acs. Nano.* **2016**, *10*, 3881.

[40] K. Huang, Q. Q. Dou, X. J. Loh, *Rsc. Adv.* **2016**, *6*, 60896.

Figure legends

Figure 1. Schematic illustration of activation of OptoTrkA in HSCs. A) OptoTrkA-transfected HSCs and control HSCs were cultured in a 12-well plate which was placed on the LED light box. Light illumination was set to a 10-min-on, 50-min-off cycle. B) HSCs were isolated from the bulge region of mouse vibrissa hair follicles. C) Upon blue light illumination, the photosensitive protein, AuLOV dimerizes TrkA-ICD, which leads to activation of TrkA signaling as detected by autophosphorylation. D) The function of OptoTrkA in regulating the proliferation, migration and neural differentiation of HSCs was investigated in this study.

Figure 2. Primary culture of HSCs from hair follicle explant. A) The whisker pads of the adult mouse were dissected (i) and placed in PBS under a stereoscopic microscope (ii). Single hair follicles are then isolated (iii). A single bulge explant for culture was obtained by removing the connective tissue capsule (iv). B) The explant isolated from the mouse vibrissa hair follicles of postnatal mice is cultured on collagen type-I coated coverslips. The HSCs migrate from hair follicle explant on approximately Day 2 and the explant was removed on Day 4. Hereafter, the HSCs population was expanded for a subsequent 3 days before passaging. Scale bar: 200 μm. C) After the bulge explants were removed, the cells were stained for the expression of Nestin, Sox10 and $p75^{NTR}$. Scale bar: 20 μm. D) After sub-culturing, HSCs were found to be Nestin and Oct4 double immunoreactive. Scale bar: 100 μm. E) The expression of *Oct4*, *Sox2*, *Nanog*, *Nes*, *Sox9*, *Sox10* and *Ngfr* was determined by reverse-transcription PCR.

Figure 3. Light-induced activation of OptoTrkA promotes proliferation and migration of HSCs. A) Immunofluorescence staining of BrdU in OptoTrkA-transfected HNCSs and sham-transfected HNCSs with or without continuous 12h cyclic blue light illumination. Scale bar: 100 μm. B) Bar chart showing the average percentage of BrdU-positive HSCs. Kruskal–Wallis test followed with multiple comparisons by Dunn's test, *P<0.05, n=4. C) Wound healing assays demonstrating that the gap area covered by migrating HSCs with light-activated TrkA (OptoTrkA-light) is larger than other control groups at 12h and 24h. Scale bar: 100 μm. D) Line graph showing the percentage of the gap area covered by migrating HSCs during the wound healing assay. Kruskal–Wallis test followed with multiple comparisons by Dunn's test, *P<0.01, **P<0.01, n=10. E) Bar chart showing that the average distance of each cell to its nearest neighbor in the OptoTrkA-light group is longer as compared to the cells in other control groups. Kruskal–Wallis test followed

with multiple comparisons by Dunn's test, **P<0.01, n=10.

Figure 4. Light-induced activity of OptoTrkA promotes neuronal cell differentiation of HSCs. A) Photomicrographs showing Tuj1 immunofluorescence staining of the neuronal differentiated HSCs with and without OptoTrkA activity. Scale bar: 100 μm. B) A bar chart showing the percentage of Tuj1 immunoreactive cells. Kruskal–Wallis test followed with multiple comparisons by Dunn's test, **P<0.01, n=4. C) Bar chart showing the percentage of the cells with fibrous morphology among Tuj1 immunoreactive cells. Kruskal–Wallis test followed with multiple comparisons by Dunn's test, **P<0.01, n=4. D) Photomicrographs showing PGP9.5 immunofluorescence staining of neuronal-differentiated HSCs with and without OptoTrkA activity. Scale bar: 100 μm. E) Bar chart showing the percentage of PGP9.5 immunoreactive cells. Kruskal–Wallis test followed with multiple comparisons by Dunn's test, *P<0.01, n=4. F) Bar chart showing the percentage of the cells with fibrous morphology among PGP9.5 immunoreactive cells (n=4). Kruskal–Wallis test followed with multiple comparisons by Dunn's test, **P<0.01, n=4. The relative quantifications are normalized to the leftmost group (as control) and compared between each group for significance analysis.

Figure 5. Light-induced activity of OptoTrkA promotes glial cell differentiation of HSCs. A) Photomicrographs showing Fabp7 immunofluorescence staining of glial-differentiated HSCs with and without OptoTrkA activity. Scale bar: 100 μm. B) Bar chart showing the percentage of Fabp7 immunoreactive cells. Kruskal–Wallis test followed with multiple comparisons by Dunn's test, *P<0.01, n=4. C) Bar chart showing the relative immunofluorescence intensity of Fabp7 normalized to DAPI. Kruskal–Wallis test followed with multiple comparisons by Dunn's test,

***P<0.01, n=4. D) Photomicrographs showing S100b immunofluorescence staining of glial differentiated HSCs with and without OptoTrkA activity. Scale bar: 100 μm. E) Bar chart showing the percentage of S100b immunoreactive cells. Kruskal–Wallis test followed with multiple comparisons by Dunn's test, **P<0.01, n=4. F) Bar chart showing the relative immunofluorescence intensity of S100b normalized to DAPI. Kruskal–Wallis test followed with multiple comparisons by Dunn's test, *P<0.01, n=4. The relative quantifications are normalized to the leftmost group (as control) and compared between each group for significance analysis.

Figure 6. **Light-induced OptoTrkA activation increased the phosphorylation of ERK1/2 and AKT.** A) OptoTrkA-transfected HEK293T cells and control cells were cultured in a 12-well plate which was placed on an LED light box. Light illumination was set to a 10-min-on, 50-min-off cycle. B) Western blotting showed that cells with OptoTrkA transfection display increased phosphorylation of ERK1/2 and AKT activation when exposed to blue light for 12 hours. C) and D) Bar charts demonstrate quantifications of relative intensities of the western blotting in (B). Kruskal–Wallis test followed with multiple comparisons by Dunn's test, *p<0.01, n=3. E) Western blotting showed that cells with OptoTrkA transfections display no significant difference compared to controls when continuously illuminated with cyclic blue light for 12 hours and placed in the dark for another 24 hours. F) and G) Bar charts demonstrate quantifications of relative intensities of the western blotting in (E). Kruskal–Wallis test, P>0.05, n=3. Quantifications of Western blots are first normalized to the extreme left group (controls) and compared to each group for significance analysis.

Supplementary figure 1. Immunofluorescent staining of Map2 and GFAP. A) Photomicrographs showing Map2 immunofluorescence staining of the neuronal differentiated HSCs with or without OptoTrkA activity. Scale bar: 50 μm. B) A bar chart showing the percentage of Map2 immunoreactive cells. Kruskal–Wallis test, $P>0.05$, n=4. C) Photomicrographs showing GFAP immunofluorescent staining of glial-differentiated HSCs with or without OptoTrkA activity. Scale bar: 50 μm. D) Bar chart showing the percentage of GFAP immunoreactive cells. Kruskal–Wallis test, $P>0.05$, n=4. E) Bar chart showing the relative immunofluorescence intensity of GFAP normalized to DAPI. Kruskal–Wallis test followed with multiple comparisons by Dunn's test, $*P<0.01$, n=4. The relative quantifications are normalized to the leftmost group (as control) and compared between each group for significance analysis.

Supplementary figure 2. Activation of OptoTrkA did not induce apoptosis or cell death. A) TUNEL staining of OptoTrkA activated HSCs and control HSCs. Arrows indicated the TUNEL positive cells. Scale bar: 100 μm. B) Immunofluorescence staining of Caspase-3 (Casp3) of OptoTrkA activated HSCs and control HSCs. Arrows indicated the Casp3 immunoreactive cells. Scale bar: 100 μm.

479 Figure 1

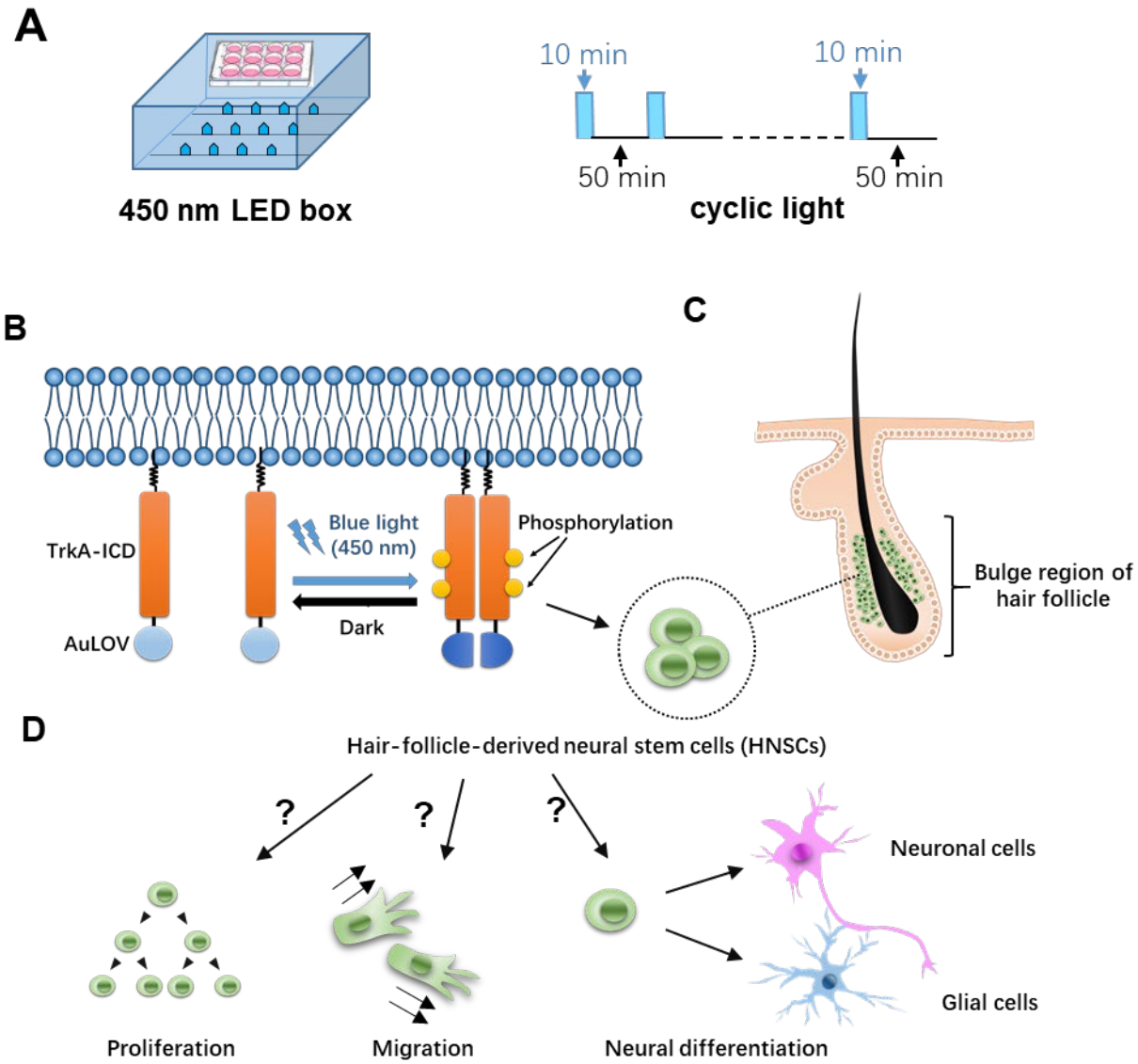

480

481 Figure 2

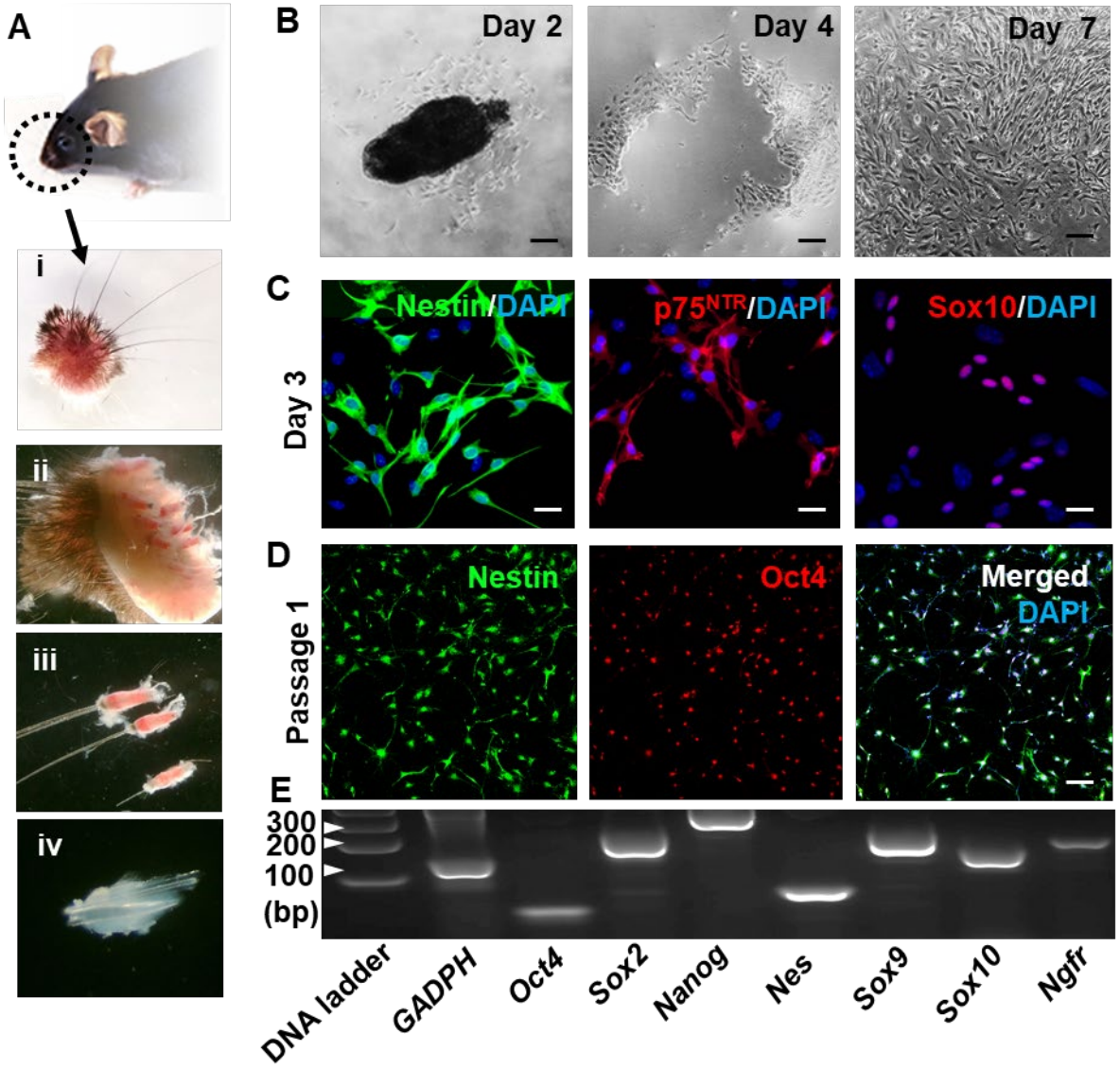

482

Figure 3

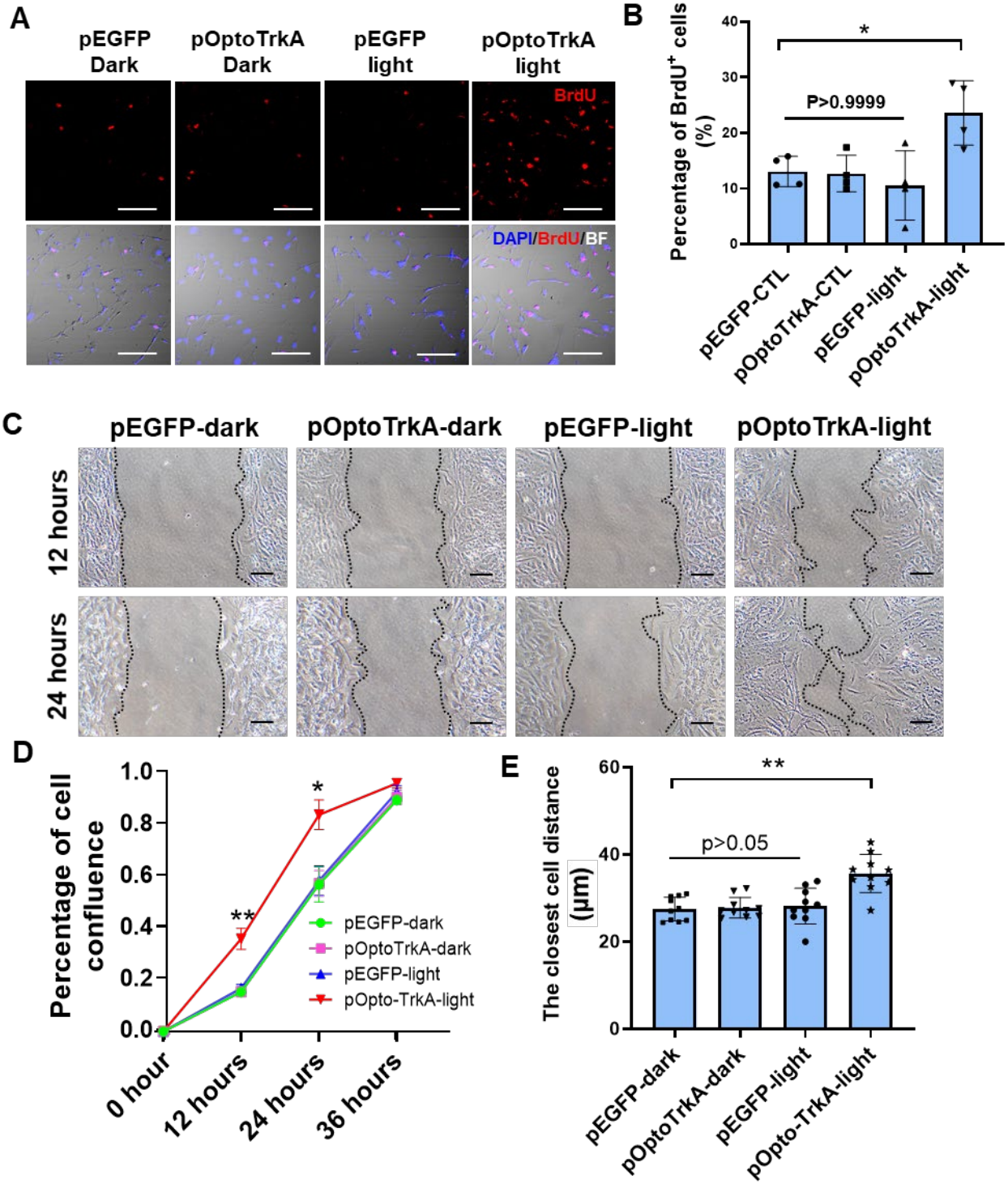
A
pEGFP Dark
pOptoTrkA Dark
pEGFP light
pOptoTrkA light
BrdU
DAPI/BrdU/BF
B
Percentage of BrdU+ cells (%)
P>0.9999
*
pEGFP-CTL
pOptoTrkA-CTL
pEGFP-light
pOptoTrkA-light
C
pEGFP-dark
pOptoTrkA-dark
pEGFP-light
pOptoTrkA-light
12 hours
24 hours
D
Percentage of cell confluence
pEGFP-dark
pOptoTrkA-dark
pEGFP-light
pOpto-TrkA-light
0 hour
12 hours
24 hours
36 hours
E
The closest cell distance (μm)
p>0.05
**
pEGFP-dark
pOptoTrkA-dark
pEGFP-light
pOpto-TrkA-light

485 Figure 4

486

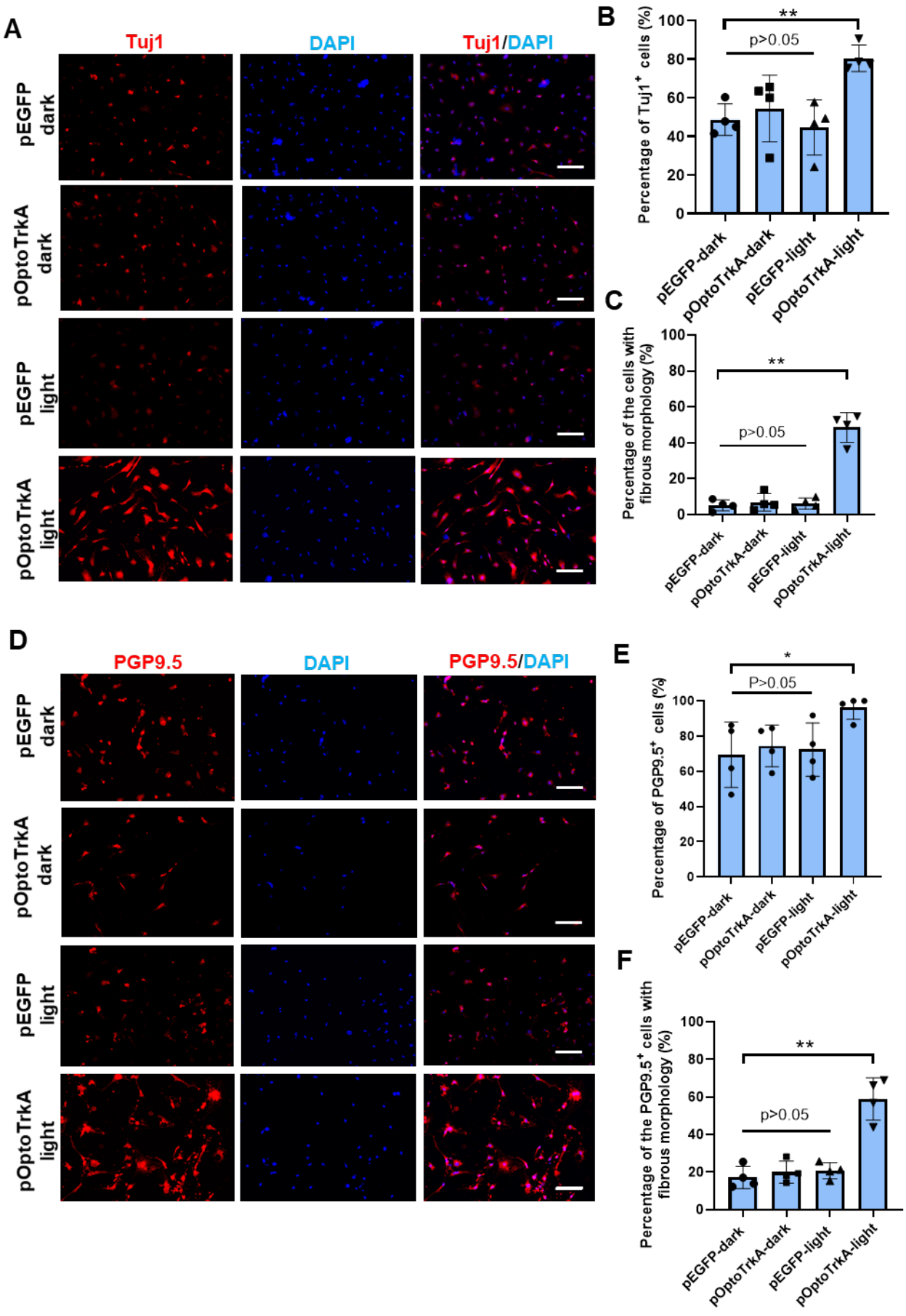

487 Figure 5

488

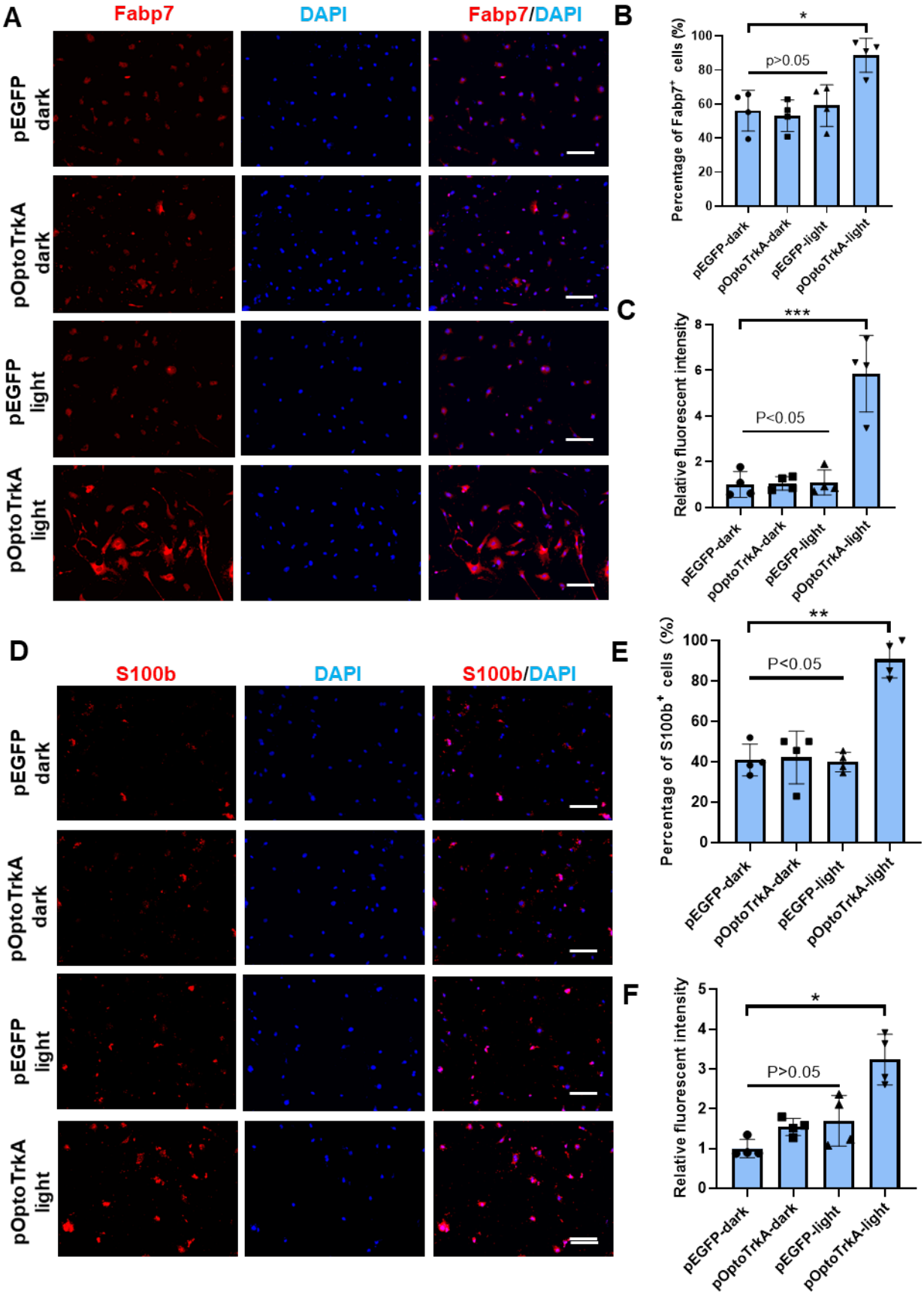

Figure 6

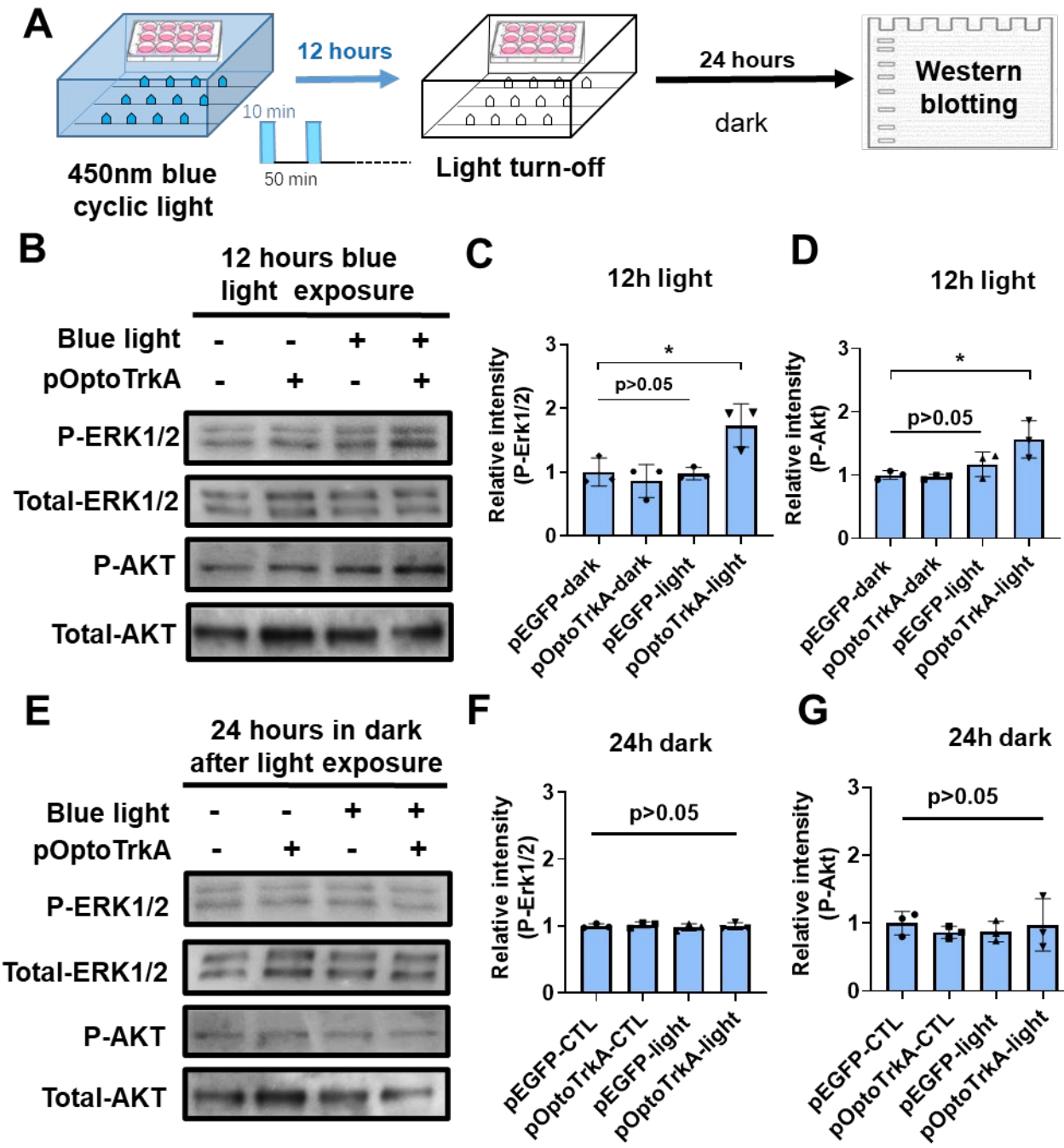
A
12 hours
10 min
50 min
450nm blue
cyclic light
Light turn-off
24 hours
dark
Western
blotting
B
12 hours blue
light exposure
Blue light - - + +
pOptoTrkA - + - +
P-ERK1/2
Total-ERK1/2
P-AKT
Total-AKT
C
12h light
Relative intensity
(P-Erk1/2)
p>0.05
*
pEGFP-dark
pOptoTrkA-dark
pEGFP-light
pOptoTrkA-light
D
12h light
Relative intensity
(P-Akt)
p>0.05
*
pEGFP-dark
pOptoTrkA-dark
pEGFP-light
pOptoTrkA-light
E
24 hours in dark
after light exposure
Blue light - - + +
pOptoTrkA - + - +
P-ERK1/2
Total-ERK1/2
P-AKT
Total-AKT
F
24h dark
Relative intensity
(P-Erk1/2)
p>0.05
pEGFP-CTL
pOptoTrkA-CTL
pEGFP-light
pOptoTrkA-light
G
24h dark
Relative intensity
(P-Akt)
p>0.05
pEGFP-CTL
pOptoTrkA-CTL
pEGFP-light
pOptoTrkA-light

492 Table 1. List of Antibodies

493

Antibody target	Species	Supplier & Cat. No.	Dilution
Nestin	Mouse	Millipore, MAB353	1:500
$p75^{NTR}$	Rabbit	Abcam, ab52987	1:300
Sox10	Rabbit	Abcam, ab27655	1:300
Oct4	Rabbit	Santa Cruz, sc-9081	1:500
Tuj1	Rabbit	Biolegend, 802001	1:500
PGP9.5	Guinea pig	Abcam, ab10410	1:500
Fabp7	Rabbit	Abcam, ab32423	1:300
S100b	Mouse	BD, BD612376	1:500
BrdU	Mouse	Roche, 11170376001	1:500
Erk1/2	Rabbit	CST, 9102	1:2000
P-Erk1/2	Rabbit	CST, 9101	1:2000
Akt	Rabbit	CST, 9272	1:2000
P-Akt	Rabbit	CST, 4060	1:2000
Donkey anti-mouse-Alexa Fluor 488/555	Donkey	Invitrogen, A21202/A31570	1:300
Donkey anti-rabbit-Alexa Fluor 488/555	Donkey	Invitrogen, A21202/A31570	1:300
Goat anti-rabbit-Alexa Fluor 555	Goat	Invitrogen, A21435	1:300
Goat anti-rabbit-HRP	Goat	Invitrogen, 656120	1:10000

494

Table 2. Primers sequences

Gene name	Forward (5'-3')	Revese (5'-3')
Gapdh	CGTCCCGTAGACAAAATGGT	TTGATGGCAACAATCTCCAC
Oct4	CTTTCCCTCTGTTCCCGTCACTGCTCTG	ATGATGAGTGACAGACAGGCCAGGCTCC
Sox2	TGGTTACCTCTTCCTCCCACTCCAG	AGTTCGCAGTCCAGCCCTCACAT
Nanog	AGGGTCTGCTACTGAGATGCTCTG	CAAACCACTGGTTTTTCTGCCACCG
Nes (Nestin)	GGAGGACCAGAGGATTGTGAACC	ACTGCCATCTGCTCATTCCCTAC
Sox9	GTTGTGGAGGGTTTTAGTTTAGATA	AAAAAAAACTCAACCAAAAATAAATAATA
Sox10	CACTCTGATCCTTTCTCC	GATTGCCTCTGACTCTTT
Nfgr ($p75^{NTR}$)	ACACTGAGCGCCAGTTACG	CTGGGTGCTGGGTGTTGT

Supplementary figure 1.

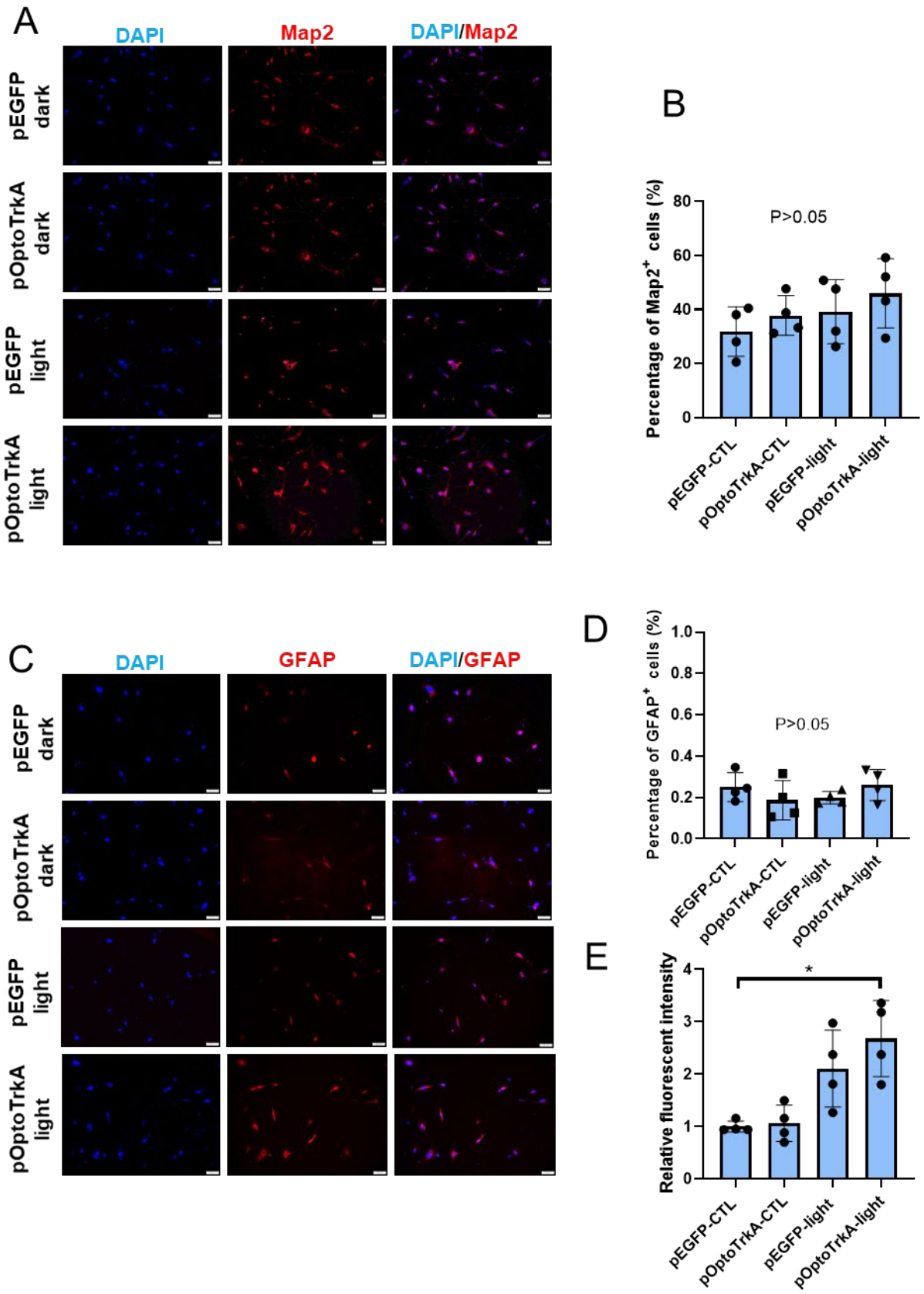

503 Supplementary figure 2.

504